



Contents lists available at ScienceDirect

Chinese Chemical Letters

journal homepage: [www.elsevier.com/locate/ccllet](http://www.elsevier.com/locate/ccllet)

# Phomaketals A and B, pentacyclic meroterpenoids from a *eupC* overexpressed mutant strain of *Phoma* sp.

Chuan Li<sup>a,1</sup>, Yangyang Han<sup>a,1</sup>, Yanan Zhai<sup>b</sup>, Ke Li<sup>a</sup>, Xingzhong Liu<sup>c</sup>, Zhuan Zhang<sup>a</sup>,  
Cai Jia<sup>a,\*</sup>, Yongsheng Che<sup>a,\*</sup>

<sup>a</sup>NHC Key Laboratory of Biotechnology of Antibiotics, Institute of Medicinal Biotechnology, Chinese Academy of Medical Sciences & Peking Union Medical College, Beijing 100050, China

<sup>b</sup>State Key Laboratory of Toxicology & Medical Countermeasures, Beijing Institute of Pharmacology & Toxicology, Beijing 100850, China

<sup>c</sup>Department of Microbiology, College of Life Sciences, Nankai University, Tianjin 300071, China

## ARTICLE INFO

### Article history:

Received 18 July 2023

Revised 27 August 2023

Accepted 30 August 2023

Available online 2 September 2023

### Keywords:

*Phoma* sp.

Tropolonic sesquiterpenes

Biosynthetic pathways

Hetero-Diels-Alder

Cytotoxicity

## ABSTRACT

Phomaketals A (**1**) and B (**2**), two tropolonic meroterpenoids with the unprecedented pentacyclic skeletons, were isolated from the solid-substrate fermentation cultures of a *eupC* overexpressed mutant strain of the fungus *Phoma* sp., together with a biogenetically related secondary metabolite pugiinin B (**3**), and the known one noreupenifeldin B (**4**). The structures of **1–3** were elucidated primarily by nuclear magnetic resonance (NMR) experiments. The absolute configurations of **1** and **2** were assigned by electronic circular dichroism calculations and the calculated NMR with DP4+ analysis, while that of **3** was established by single-crystal X-ray diffraction analysis using Cu K $\alpha$  radiation. Biogenetically, phomaketals A (**1**) and B (**2**) could be derived from the hypothetical tropolonic sesquiterpene intermediates neosetophomone B (**6**) and 9-R-neosetophomone B (**6'**), respectively, via different reactions cascades. Compound **1** showed antiproliferative effect only against the SUPB15 cells, with an 50% inhibitory concentration (IC<sub>50</sub>) value of 4.85  $\mu$ mol/L, while the co-isolated known meroterpenoid **4** displayed potent effects against three tumor cell lines, SUPB15, EL4, and H9, showing IC<sub>50</sub> values of 0.36–27.08  $\mu$ mol/L.

© 2024 Published by Elsevier B.V. on behalf of Chinese Chemical Society and Institute of Materia Medica, Chinese Academy of Medical Sciences.

Tropolonic sesquiterpenes are a class of meroterpenoids derived from the polyketide tropolone including its rearranged products, and the terpenoid humulene via intermolecular hetero-Diels-Alder reactions [1–13]. Tropolonic sesquiterpenoids can generally be grouped into three major categories based on the presence of tropolone(s) [1–6], its rearranged product(s) [4–8], or both as the polyketide counterparts of the structures [6,9–12]. Notable examples of unique tropolonic sesquiterpenes co-isolated with eupenifeldin have been reported from the species of *Phoma*, *Neosetophoma*, and *Phomopsis* [6,10–12], in which the tropolone moiety in eupenifeldin was replaced by furan-2(5H)-one, 3a,7a-dihydro-2H-furo[3,2-b]pyran-2,5(3H)-dione, and 3a,6a-dihydro-4H-cyclopenta[b]furan-4-one, respectively. Due to their diverse structure characteristics, and profound biological effects [1–18], tropolonic sesquiterpenoids have attracted much attention from synthetic chemists and biochemists [19–28].

Our prior chemical investigation of a strain of *Phoma* sp., isolated from a soil sample from the Qinghai-Tibetan plateau, Tibet, People's Republic of China, has afforded a variety of bioactive tropolonic sesquiterpenes with unique structural features [10,11]. Recently, we identified the biosynthetic gene cluster (BGC) responsible for the biosynthesis of eupenifeldin (*eup*) in *Phoma* sp., and confirmed that the oxidase *EupC*, highly homologous to *TropC* [22], catalyzed formation of the tropolone skeleton [25]. Since overexpression of key genes in BGCs has been demonstrated to be an effective approach to genetically manipulate the production of natural products, and to effectively expand structural diversities [29–31], oxidative modification of tropolone unit is expected to produce a variety of ring-contracted and other rearranged congeners. Based on this consideration, the strain *Phoma* sp. *eupCOE* was prepared by overexpressing *eupC* in the wild-type (WT) strain of *Phoma* sp. The high-performance liquid chromatography (HPLC) fingerprint of the crude extract of *Phoma* sp. *eupCOE* revealed the presence of metabolites that were different from those produced by the WT strain (Fig. S1 in Supporting information). Further chemical investigations of this extract led to the isolation of two unique tropolonic meroterpenoids that have been named phomaketals A and B, a new biogenetically related analogue pugiinin B (**1–3**; Fig. 1), and

\* Corresponding authors.

E-mail addresses: [caijia@imb.cams.cn](mailto:caijia@imb.cams.cn) (C. Jia), [ysche@imb.cams.cn](mailto:ysche@imb.cams.cn) (Y. Che).

<sup>1</sup> These authors contributed equally to this work.

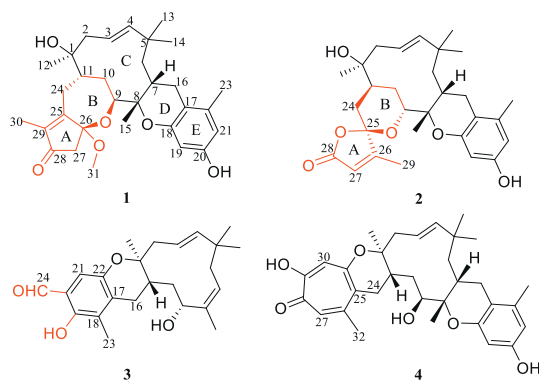


Fig. 1. Chemical structures of compounds 1–4.

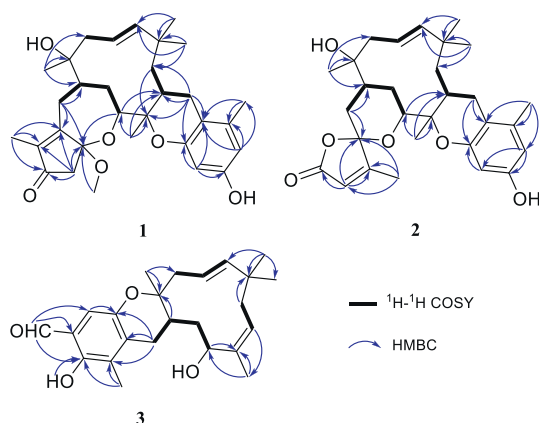


Fig. 2. Key  $^1\text{H}$ - $^1\text{H}$  COSY and HMBC correlations of 1–3.

the known noreupenifeldin B (**4**) [6]. Details of the isolation, structure elucidation, cytotoxicity evaluation, and putative biogenesis of these compounds are reported herein.

Phomaketol A (**1**) was assigned the molecular formula  $\text{C}_{31}\text{H}_{42}\text{O}_6$  (11 degrees of unsaturation) based on its high-resolution electrospray ionization mass spectrometry (HRESIMS) and nuclear magnetic resonance (NMR) data (Table S1 in Supporting information). Analysis of its NMR data revealed the presence of seven methyl groups with one *O*-methyl, six methylene units, three methines including one oxygenated, 10 olefinic/aromatic carbons with four protonated ones, four  $\text{sp}^3$  quaternary carbons (three oxygenated carbons including one with double oxygenation at  $\delta_{\text{C}}$  103.8), and an  $\alpha,\beta$ -unsaturated ketone carbon at 204.6 ppm. These data accounted for all of the NMR resonances of **1** except for two unobserved exchangeable protons, and required **1** to be a pentacyclic compound. Interpretation of the  $^1\text{H}$  and  $^{13}\text{C}$  NMR spectroscopic data for **1** revealed the presence of the same tetrahydrohumulene moiety, a dihydro-2*H*-pyran unit, and a tetrasubstituted aryl ring, corresponding to fragments C–E, respectively, as those typically found in the known compound phomanolide A [10], but the remaining portion was significantly different, warranting a detailed two-dimensional (2D) NMR analysis. Analysis of the  $^1\text{H}$ - $^1\text{H}$  correlation spectroscopy (COSY) NMR data of **1** (Fig. 2) defined three isolated spin-systems of C-2–C-4, C-6–C-16 (via C-7), and C-9–C-24 (via C-10 and C-11), HMBC correlations from  $\text{H}_3$ -12 to C-1, C-2, and C-11,  $\text{H}_3$ -13 and  $\text{H}_3$ -14 to C-4, C-5, and C-6,  $\text{H}_3$ -15 to C-7, C-8 and C-9, and from H-6a and  $\text{H}_2$ -16 to C-8 established the 11-membered humulene unit (C), and a tetrasubstituted aryl ring (E), as confirmed by the heteronuclear multiple-bond correlation (HMBC) cross-peaks from H-19 to C-17, C-18, and C-20, H-21 to C-17, C-22, and C-23, and from  $\text{H}_3$ -23 to C-17, C-21, and C-22. While

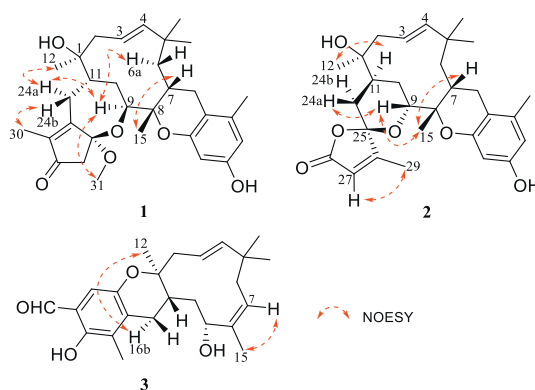


Fig. 3. Key NOESY correlations of 1–3.

those correlations of H-16a with C-6, C-7, and C-8, and of H-16b with C-8, C-17, and C-18, plus the chemical shift values for C-8 ( $\delta_{\text{C}}$  79.7) and C-18 ( $\delta_{\text{C}}$  154.6) indicated that C-8 and C-18 are both attached to the same oxygen atom to form a dihydro-2*H*-pyran ring (D). In turn, correlations from  $\text{H}_2$ -24 to C-11, C-25, and  $\text{H}_3$ -30 to C-25, C-28, and C-29, and from  $\text{H}_2$ -27 to C-25 ( $\delta_{\text{C}}$  135.6), C-26, C-28 ( $\delta_{\text{C}}$  204.6), and C-29 ( $\delta_{\text{C}}$  167.5) established a cyclopentenone ring with an  $\alpha,\beta$ -unsaturated ketone moiety (C-25–C-28 via C-29), and a methyl group located at C-29, completing the 2-methylcyclopent-2-en-1-one moiety (A), which was connected to C-11 of humulene unit (C) via C-24. The HMBC correlations from H-9 and  $\text{H}_3$ -31 to C-26, as well as the chemical shift value for C-9 ( $\delta_{\text{C}}$  70.1) and the doubly-oxygenated nature of C-26 ( $\delta_{\text{C}}$  103.8), suggested that the two C-26 attached oxygen atoms were individually connected to C-9 and C-31 to form an oxepane moiety (B) in **1**. The HMBC correlations (Table S2 in Supporting information) from the exchangeable proton at 4.59 ppm to C-1, C-2, and C-11, and from that at 8.96 ppm to C-19, C-20, and C-21, located the two free hydroxy groups at C-1 and C-20, respectively. Collectively, the gross structure of **1** was tentatively assigned as shown.

The relative configuration of **1** was deduced by analysis of the  $^1\text{H}$ - $^1\text{H}$  coupling constants and nuclear Overhauser effect spectroscopy (NOESY) data (Fig. 3). The C-3/C-4 olefin was assigned the *E*-geometry based on the large *J* value of 16.2 Hz observed for H-3/H-4. The large *trans*-diaxial type *J* values of 15.0 and 12.0 Hz for H-7/H-6a and H-11/H-24a, respectively, revealed their axial orientations [10]. NOESY correlation of  $\text{H}_3$ -30 and H-24b revealed the *Z*-geometry for C-25/C-29 olefin. Correlation of  $\text{H}_3$ -15 with H-7 indicated that these protons are on the same face of the ring system, whereas those of H-9 with H-6a, H-24a, and  $\text{H}_3$ -31 and of  $\text{H}_3$ -12 with H-24a placed them on the opposite face of the molecule. The absolute configuration of **1** was deduced by comparison of the experimental and simulated electronic circular dichroism (ECD) spectra (Fig. 4) generated by time-dependent density functional theory (TDDFT) for the (1*S*,7*R*,8*S*,9*S*,11*S*,26*S*)-**1** (**1a**) and (1*R*,7*S*,8*R*,9*R*,11*R*,26*R*)-**1** (**1b**) enantiomers [32]. The MMFF94 conformational search followed by B3LYP/6-31G(d) TDDFT reoptimization afforded seven lowest energy conformers for **1a** (Table S5 in Supporting information). The overall calculated ECD spectra of **1a** and **1b** were then generated by Boltzmann weighting of each conformer. The experimental ECD curve of **1** nearly identical to the calculated ECD spectrum of **1a**, suggesting that **1** has the 1*S*,7*R*,8*S*,9*S*,11*S*,26*S* absolute configuration.

The molecular formula of phomaketol B (**2**) was determined to be  $\text{C}_{29}\text{H}_{38}\text{O}_6$  (11 degrees of unsaturation) by its HRESIMS and the NMR data (Table S1). The  $^1\text{H}$  and  $^{13}\text{C}$  NMR spectroscopic data of **2** revealed the presence of the same partial structure (rings C–E) as that found in **1**. However, resonances for the remaining portion differed significantly from those of **1**. Detailed analysis of the

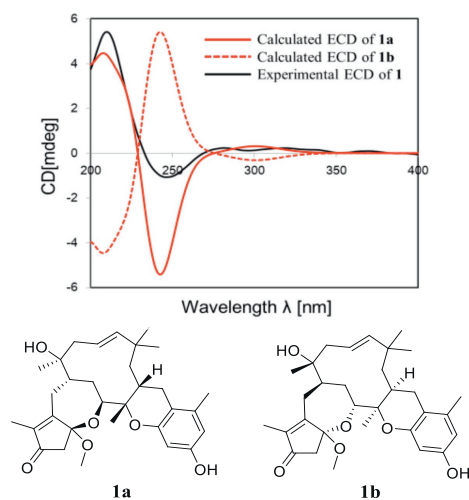


Fig. 4. Experimental ECD spectrum of **1** in MeOH and the calculated ECD spectra of **1a** and **1b** enantiomers.

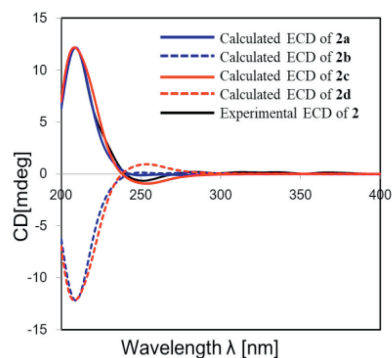


Fig. 5. Experimental ECD spectrum of **2** in MeOH and the calculated ECD spectra of **2a-d**.

2D NMR data was performed to establish the different portion of the structure. The HMBC cross-peaks from H-24a to C-25 and from H<sub>3</sub>-29 to C-25, C-26, and C-27 led to the connection of C-25 to C-24 and C-26, with the C-29 methyl group located at C-26. Correlations from the olefinic proton H-27 to C-26 and C-28 ( $\delta_C$  170.6) indicating that the carboxylic carbon C-28 is allylic to the C-26/C-27 olefin, establishing a 3-methylpent-2-enoate moiety, which was located at C-11 based on the HMBC correlation from H<sub>2</sub>-24 to C-11 and relevant <sup>1</sup>H-<sup>1</sup>H COSY NMR data. In addition, the two exchangeable protons ( $\delta_H$  4.56 and 8.95, respectively) presented in **2** were individually assigned to the free hydroxy groups attached to C-1 and C-20 by relevant HMBC correlations (Table S2). Considering the unsaturation requirement, the chemical shifts values for the C-9 oxymethine carbon ( $\delta_C$  75.7) and C-28 carboxylic carbon ( $\delta_C$  170.6), plus the doubly oxygenated nature of C-25 ( $\delta_C$  109.3), the two C-25 bonded oxygen atoms were each connected to C-9 and C-28 by default to complete the 4-methyl-1,6-dioxaspiro[4.5]dec-3-en-2-one moiety (A and B), even though no additional evidence for these linkages was provided by the HMBC data. Collectively, the gross structure of **2** was established as shown.

The relative configuration of **2** was also proposed on the basis of the <sup>1</sup>H-<sup>1</sup>H *J* values and NOESY data. The C-3/C-4 olefin was assigned the *E*-geometry by the large *J* value observed for H-3/H-4 (15.6 Hz). NOESY cross-peaks of H-7/H<sub>3</sub>-15/H-9/H-24a placed these protons on the same face of molecule, while the large *trans*-diaxial type *J* value of 13.2 Hz for H-11/H-24a, and a NOESY cross-peak of H-11/H<sub>3</sub>-12 revealed opposite orientation for these protons. Additional correlations of H<sub>3</sub>-29 with H-27 allowed assignment of the *Z*-geometry for the C-26/C-27 olefin. The absolute configuration of **2** was proposed by comparison of the experimental and simulated ECD spectra. The ECD spectra of four isomers (**2a-d**; Fig. 5) were calculated to represent all the possible configurations, and the experimental ECD spectrum of **2** reasonably agreed with that calculated for **2c** (Tables S6 and S7 in Supporting information), suggesting the 1*S*,7*R*,8*S*,9*R*,11*S*,25*R* absolute configuration. To validate the configuration of C-25, the <sup>13</sup>C NMR chemical shifts of **2a** and **2c** (Tables S8 and S9 in Supporting information), showing similar ECD spectra, were calculated using the gauge-including atomic orbitals (GIAO) method [33]. The root-mean-square error (RMSE) between experimental and the calculated <sup>13</sup>C NMR data and the DP4+ probability analysis revealed 100% probability of the 25*R*-configuration for **2c** (Table S11 in Supporting information). And based on the coefficient values, **2c** was the best match ( $R^2 = 0.9965$ ; Fig. S29

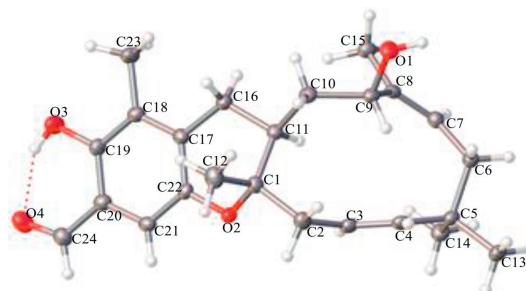
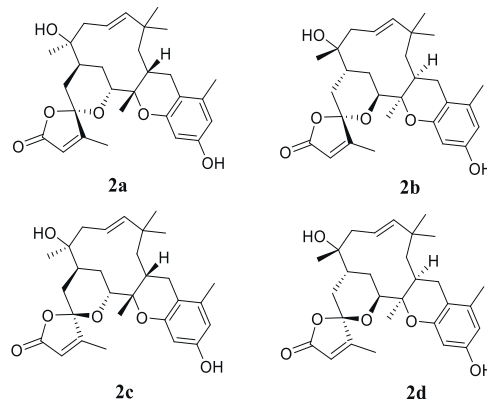
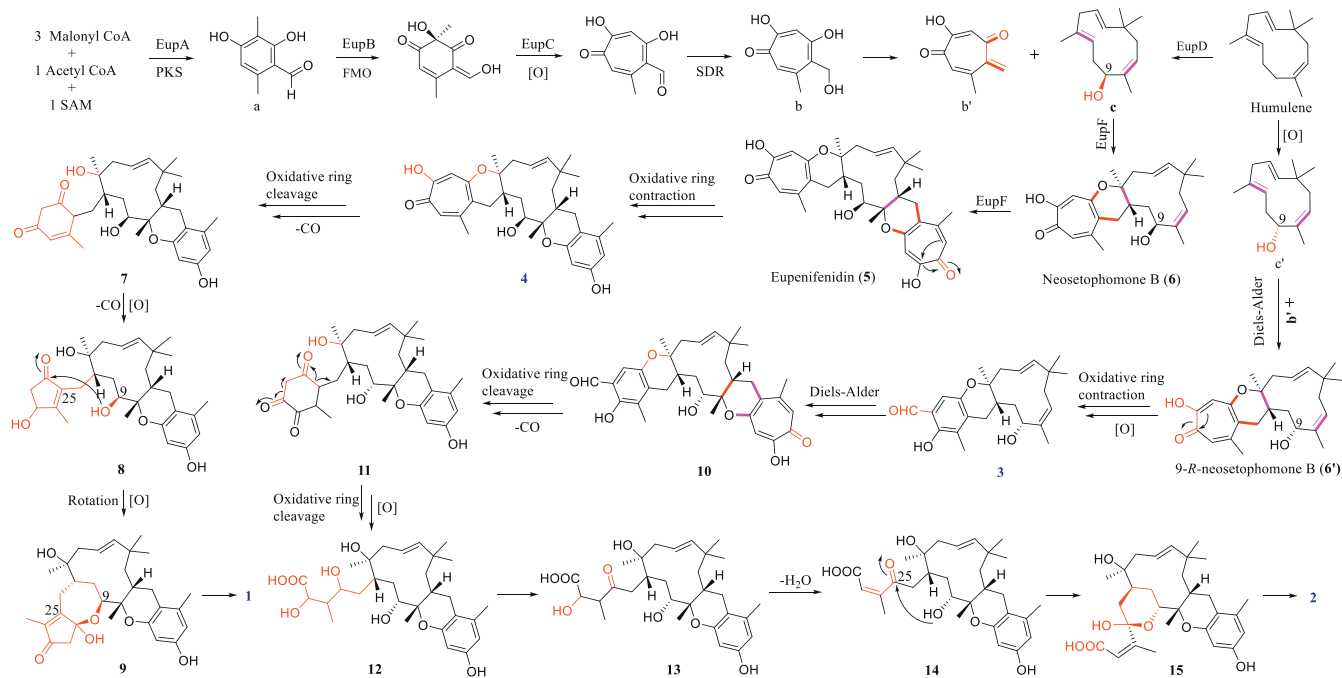


Fig. 6. Thermal ellipsoid representation of **3** (the ellipsoid contour probability level is 50%).

in Supporting information), supporting the absolute configuration proposed for **2** by ECD calculations. Therefore, the absolute configuration of **2** was established as 1*S*,7*R*,8*S*,9*R*,11*S*,25*R*.

The molecular formula of pughinin B (**3**) was established as C<sub>24</sub>H<sub>32</sub>O<sub>4</sub> by HRESIMS. Analysis of its <sup>1</sup>H and <sup>13</sup>C NMR spectroscopic data (Table S3 in Supporting information) revealed structural similarity to those of the known metabolite pughinin A [7], except that the chemical shift of C-19 ( $\delta_C$  108.7) was shifted significantly downfield to 152.9 ppm, and the resonances for C-20 and attached hydroxy proton were replaced by those for an aldehyde functionality ( $\delta_H/\delta_C$  9.73/196.1) in **3**. These observations were supported by the HMBC correlations of OH-19 with C-19 and C-20, and of H-24 with C-19, C-20, and C-21, allowing assignment of the gross structure of **3** as shown. The relative configuration of **3** was deduced on the basis of the <sup>1</sup>H-<sup>1</sup>H coupling constants and NOESY data (Fig. 3), and was further confirmed by X-ray crystallography using Cu K $\alpha$  radiation (Fig. 6) (CCDC: 2239679), from which the absolute configuration was determined to be 1*S*,9*R*,11*S* based on the value of the Flack parameter,  $-0.04(4)$ .

Compound **4** was readily identified as noreupenifeldin B by comparison of its optical rotation value, HRESIMS, and NMR data



Scheme 1. Hypothetical biosynthetic pathways for 1–4.

Table 1  
Cytotoxicity of compounds 1–4.

Compound	IC <sub>50</sub> (μmol/L)		
	SUPB15	EL4	H9
<b>1</b>	4.85 ± 0.49	>100	>100
<b>2</b>	>100	>100	>100
<b>3</b>	>100	36.87 ± 0.88	>100
<b>4</b>	27.08 ± 0.10	0.36 ± 0.03	4.37 ± 0.58
Daunorubicin <sup>a</sup>	(18.38 ± 0.78) × 10 <sup>-3</sup>	(72.61 ± 0.46) × 10 <sup>-3</sup>	(272.20 ± 1.17) × 10 <sup>-3</sup>

<sup>a</sup> Positive control.

(Table S4 in Supporting information) with those reported [6,26]. Although its relative configuration was first assigned by NOESY data [6], and later reported from other fungus [26], its absolute configuration remained unassigned. To correlate biogenesis of the co-isolated metabolites, it is necessary to assign its absolute configuration, which was deduced in the current work by comparison of the experimental and calculated ECD spectra for (1*S*,7*R*,8*S*,9*S*,11*S*)-**4** (**4a**) and (1*R*,7*S*,8*R*,9*R*,11*R*)-**4** (**4b**) conformers (Fig. S30 in Supporting information). The MMFF94 conformational search and TDDFT reoptimization at the B3LYP/6–31G(d) basis set level afforded two lowest energy conformers for **4a** (Table S13 in Supporting information). The experimental ECD spectrum of **4** was nearly identical to that calculated for **4a**, suggesting the 1*S*,7*R*,8*S*,9*S*,11*S* absolute configuration.

Compounds **1–4** were evaluated for antiproliferative effects against three tumor cell lines, SUPB15 (human acute lymphocyte leukemia), EL4 (mouse lymphoma cells), and H9 (human T lymphoma leukemia) (Table 1). Compound **1** showed activity only against SUPB15 cells, with an 50% inhibitory concentration (IC<sub>50</sub>) value of 4.85 μmol/L, **2** did not show detectable activity at 100 μmol/L, **3** was active toward EL4 cells, with an IC<sub>50</sub> value of 36.87 μmol/L. Compound **4** displayed the expected activity against all three tumor cell lines, with IC<sub>50</sub> values of 0.36–27.08 μmol/L, while the positive control daunorubicin showed IC<sub>50</sub> values of 18.38–272.20 nmol/L.

Although several natural products showing partial structural similarity to phomaketals A (**1**) and B (**2**) have been reported [10–12], compounds **1** and **2** are new and unique additions of the tropolonic meroterpenoid class of compounds possessing the unprecedented pentacyclic skeletons. Compound **1** possesses a unique 5/7/11/6/6 skeleton with the rare 2,3,4,5,8,8a-hexahydro-7*H*-cyclopenta[*b*]oxepin-7-one moiety, with a thiophene isolated from the plant *Artemisia rupestris* as the only precedent incorporating the same unit [34]. While compound **2** possesses an unprecedented C-25-spiro-fused 5/6/11/6/6 pentacyclic core incorporating a rare 1,6-dioxaspiro[4.5]dec-3-en-2-one unit, with fungal natural products sequoiamonacins A and B [35] and talaromyacins A–C [36], and plant metabolites spirochensilides A and B [37] as the precedents incorporating this moiety. To our knowledge, compounds **1** and **2** are the first examples of oxidative modification of the tropolone and pyran moieties (B) that are fused to the humulene (C) at C-9/C-11. Compound **3** is a new tropolonic meroterpenoid with an aldehyde functionality, and its absolute configuration was assigned for the first time by X-ray crystallography. In addition, the absolute configuration of the known noreupenifeldin B (**4**) was proposed for the first time by ECD calculations. Biogenetically, tropolone orthoquinone methide (**b'**) and humulene (**c** and **c'**) could be the biosynthetic precursors for **1–4** (Scheme 1), first undergo a hetero-Diels-Alder reaction to form the key intermediates neosetophomone B (**6**) [6,24] and 9-*R*-neosetophomone B (**6'**), and followed by reactions including hetero-Diels-Alder reaction, oxidative ring-contraction and -cleavage [4–6], rearrangement [10–12], and lactonization via different routes to form **1–4** [22–28]. These results have further demonstrated the feasibility for generation of structurally unique and diverse tropolonic meroterpenoids by manipulating the key biosynthetic genes.

#### Declaration of competing interest

The authors declare that they have no known competing financial interests or personal relationships that could have appeared to influence the work reported in this paper.

## Acknowledgments

We gratefully acknowledge financial support from the National Natural Science Foundation of China (No. 82003628) and the CAMS Innovation Fund for Medical Sciences (Nos. 2021-I2M-1-030, 2021-I2M-1-028, and 2021-1-I2M-2-002).

## Supplementary materials

Supplementary material associated with this article can be found, in the online version, at doi:10.1016/j.ccllet.2023.109019.

## References

- [1] F. Mayerl, Q. Gao, S. Huang, et al., *J. Antibiot.* 46 (1993) 1082–1088.
- [2] G.H. Harris, K. Hoogsteen, K.C. Silverman, *Tetrahedron* 49 (1993) 2139–2144.
- [3] P. Cai, D. Smith, B. Cunningham, et al., *J. Nat. Prod.* 61 (1998) 791–795.
- [4] M.E. Raggatt, T.J. Simpson, M.I. Chicarelli-Robinson, *Chem. Commun.* (1997) 2245–2247.
- [5] S. Ayers, D.L. Zink, J.S. Powell, et al., *J. Nat. Prod.* 71 (2008) 457–459.
- [6] T. El-Elmat, H.A. Raja, S. Ayers, et al., *Org. Lett.* 21 (2019) 529–534.
- [7] P. Pittayakhajonwut, M. Theerasilp, P. Kongsaree, et al., *Planta Med.* 68 (2002) 1017–1019.
- [8] T. Bunyapaiboonsri, S. Veeranondha, T. Boonruangprapa, S. Somrithipol, *Phytochem. Lett.* 1 (2008) 204–206.
- [9] A.M. Ainsworth, M.I. Chicarelli-Robinson, B.R. Copp, et al., *J. Antibiot.* 48 (1995) 568–573.
- [10] J. Zhang, L. Liu, B. Wang, et al., *J. Nat. Prod.* 78 (2015) 3058–3066.
- [11] J. Zhang, Y. Li, F. Ren, et al., *J. Nat. Prod.* 82 (2019) 1678–1685.
- [12] S. Chen, Z. Liu, H. Tan, et al., *Org. Chem. Front.* 7 (2020) 557–562.
- [13] L. Li, R.J. Cox, *J. Fungi* 8 (2022) 929.
- [14] C.J. Hsiao, S.H. Hsiao, W.L. Chen, et al., *Chem. Interact.* 197 (2012) 23–30.
- [15] Z.Y.A. Subeh, N.Q. Chu, J.T. Korunes-Miller, et al., *J. Control. Release* 331 (2021) 260–269.
- [16] M. Kaneko, D. Matsuda, M. Ohtawa, *Biol. Pharm. Bull.* 35 (2012) 18–28.
- [17] D.P. Overy, F. Berrue, H. Correa, et al., *Mycology* 5 (2014) 130–144.
- [18] A.D. Wright, N. Lang-Unnasch, *Planta Med.* 71 (2005) 964–966.
- [19] R.M. Adlington, J.E. Baldwin, A.V.W. Mayweg, G.J. Pritchard, *Org. Lett.* 4 (2002) 3009–3011.
- [20] P.J. Li, G. Drager, A. Kirschning, *Org. Lett.* 21 (2019) 998–1001.
- [21] C.Y. Bemis, C.N. Ungarean, A.S. Shved, et al., *J. Am. Chem. Soc.* 143 (2021) 6006–6017.
- [22] J. Davison, A. Al-Fahad, M. Cai, et al., *Proc. Natl. Acad. Sci. U. S. A.* 109 (2012) 7642–7647.
- [23] R. Schor, C. Schotte, D. Wibberg, J. Kalinowski, R.J. Cox, *Nat. Commun.* 9 (2018) 1963.
- [24] Q. Chen, J. Gao, C. Jamieson, et al., *J. Am. Chem. Soc.* 141 (2019) 14052–14056.
- [25] Y. Zhai, Y. Li, J. Zhang, et al., *Fung. Genet. Biol.* 129 (2019) 7–15.
- [26] C. Schotte, L. Li, D. Wibberg, J. Kalinowski, R.J. Cox, *Angew. Chem. Int. Ed.* 59 (2020) 23870–23878.
- [27] C. Schotte, P. Lukat, A. Deuschmann, W. Blankenfeldt, R.J. Cox, *Angew. Chem. Int. Ed.* 60 (2021) 20308–20312.
- [28] J. Liu, J. Lu, C. Zhang, et al., *Nat. Chem.* 15 (2023) 1083–1090.
- [29] B. Zhang, W. Tian, S. Wang, et al., *ACS Chem. Biol.* 12 (2017) 1732–1736.
- [30] F. Wei, Z. Wang, C. Lu, et al., *Org. Lett.* 21 (2019) 7818–7822.
- [31] L. Dai, Z. Wang, H. Wang, C.H. Lu, Y.M. Shen, *Chin. J. Nat. Med.* 18 (2020) 952–956.
- [32] C.Y. Zhang, Y.L. Li, Z.J. Chu, et al., *Chin. Chem. Lett.* 35 (2024) 108206.
- [33] Y. Feng, S. Zha, H. Zhang, et al., *Chin. Chem. Lett.* 34 (2023) 107742.
- [34] Y. Cao, Y. Zang, X. Huang, Z.H. Cheng, *Nat. Prod. Res.* 35 (2021) 1775–1782.
- [35] D.B. Stierle, A.A. Stierle, T. Bugni, *J. Org. Chem.* 68 (2003) 4966–4969.
- [36] X. Cao, Y.C. Ge, D.H. Lan, X.D. Wu, B. Wu, *Fitoterapia* 164 (2023) 105359.
- [37] Q.Q. Zhao, Q.Y. Song, K. Jiang, et al., *Org. Lett.* 17 (2015) 2760–2763.